JOURNAL OF Materials CHEMISTRY

Structures and magnetic ordering in the brownmillerite phases, Sr_2MnGaO_5 and Ca_2MnAlO_5

A. J. Wright, H. M. Palmer, P. A. Anderson and C. Greaves*

School of Chemical Sciences, University of Birmingham, Birmingham, UK B15 2TT. E-mail: c.greaves@bham.ac.uk

Received 29th October 2001, Accepted 14th February 2002
First published as an Advance Article on the web 5th March 2002

The crystal and magnetic structures of the two related phases, Sr_2MnGaO_5 and Ca_2MnAlO_5 are reported. Rietveld analysis of neutron powder diffraction has revealed that both phases adopt the brownmillerite structure. Subtle differences in structure lead to the structure of Sr_2MnGaO_5 being best described by the space group *Icmm* (a = 5.4888(2) Å, b = 16.2256(6) Å, c = 5.35450(2) Å at 2 K) while that of Ca_2MnAlO_5 is best described by *Ibm*2 (a = 5.46258(9) Å, b = 14.9532(3) Å, c = 5.23135(8) Å at 2 K). Low temperature neutron powder diffraction data show that both phases have a simple antiferromagnetic structure. However, magnetisation data suggest a more complex picture of the magnetic order within these phases.

Introduction

Layered manganese oxide materials are of great interest due to their potential as low field colossal magnetoresistance (CMR) materials. The CMR effect is well documented in manganese oxide perovskite phases and much of the work in this field has focussed on these materials. At present one of the fundamental problems with these phases is the impractically high magnetic fields required for the highest CMR effects to be observed. However, the observation of a CMR effect at much lower fields in a Ruddlesden–Popper phase ($La_{1.2}Sr_{1.8}Mn_2O_7$),[1,2] has led to the suggestion that lower dimensional phases (such as those with the two-dimensional Ruddlesden–Popper structures) may have potential as low field CMR materials. We have therefore investigated the synthesis of new low-dimensional manganese-containing materials and have previously communicated the synthesis of the brownmillerite phase, Sr_2MnGaO_5.[3] The brownmillerite structure is a two-dimensional, oxygen-deficient variant of perovskite, and is therefore closely related to the simple structures of the manganese perovskites, which show good CMR properties, *e.g.* $La_{1-x}Ca_xMnO_3$. The brownmillerite structure is adopted by, for example, $Ca_2Fe_2O_5$,[4,5] $Sr_2Fe_2O_5$,[6,7] and $Ca_2(Fe,Al)_2O_5$,[4,8] and comprises alternating layers of cations in octahedral and tetrahedral coordination. Sr_2MnGaO_5 contains layers of octahedral Mn ions interleaved with layers of tetrahedral Ga ions. The oxygen vacancies within the GaO layers are ordered such that chains of corner linked GaO_4 tetrahedra are formed (see Fig. 1). It is subtleties in the relative displacements of the atoms in these chains which are known to lead to brownmillerite phases crystallising in one of three possible space groups *Icmm*, *Ibm*2 or *Pcmn*.[5,6] As discussed later, whereas *Ibm*2 and *Pcmn* describe fully ordered structures, *Icmm* corresponds to incomplete order of the cation and oxygen displacements. Our preliminary study of the structure of Sr_2MnGaO_5, using X-ray powder diffraction data, concluded that *Icmm* was the preferred space group.[3] However, a recent report by Abakumov *et al.*,[9] also using X-ray powder diffraction data, suggested a different space group, *Ima*2 (equivalent to *Ibm*2), for this phase. It is important that such a discrepancy is investigated and therefore we report here a detailed structural study of Sr_2MnGaO_5 using neutron diffraction data to fully determine the relative nature of the GaO_4 chain orientations in this phase. Since oxygen displacements are primarily involved, the greater sensitivity of neutron diffraction provides a much more accurate and reliable means of determining such detail. Our results are also compared with those recently reported for $Ca_2MnGa_{1-x}Zn_xO_{5+\delta}$.[10]

In addition, we report fully on the magnetic properties of Sr_2MnGaO_5 and compare the structural and magnetic properties of Sr_2MnGaO_5 with those of Ca_2MnAlO_5, which we demonstrate to be a closely related brownmillerite phase. Although a phase with the formula Ca_2MnAlO_5 has previously been reported to crystallise with an orthorhombic structure similar to that of Ca_2AlFeO_5,[11] a full structure determination has not been carried out.

Experimental

Sr_2MnGaO_5 was synthesised by firing an intimate mixture of stoichiometric quantities of high purity $SrCO_3$, Ga_2O_3 and Mn_2O_3 at 1350 °C for 48 h in flowing nitrogen. Similarly,

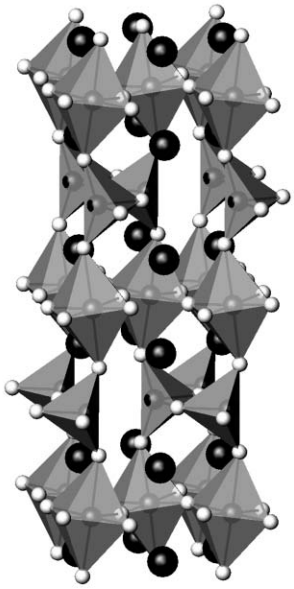

Fig. 1 Structure of Sr_2MnGaO_5 showing Sr (large black spheres) with MnO_6 octahedral layers alternating with layers of GaO_4 tetrahedra. (This representation is based on the fully ordered *Ibm*2 structure to aid clarity.)

 DOI: 10.1039/b109865a

Ca_2MnAlO_5 was synthesised from high purity $CaCO_3$, Al_2O_3 and Mn_2O_3, but was fired at a slightly lower temperature (1250 °C for 48 h in flowing nitrogen). Both phases were subjected to further firings under similar conditions until phases with oxygen contents close to 5.0 were obtained. The oxygen content of each phase was initially determined *via* thermogravimetric analysis (reduction in 10% H_2/N_2 using a Rheometric Scientific STA 1500 thermal analyser). X-ray powder diffraction (Siemens D5000, PSD, Ge monochromator providing Cu $K\alpha_1$) was also used to confirm single phase products had been synthesised. Neutron powder diffraction (NPD) data were collected for both phases at 300 K and 2 K on the POLARIS diffractometer at RAL, Oxfordshire, UK, and Rietveld analyses of these data were carried out using the GSAS suite of programs.[12] Hartree–Fock magnetic form factors were used for the Mn^{3+} ions.[13] Magnetic measurements were obtained using a Cryogenics S100 dc SQUID magnetometer (susceptibility *versus* temperature at 500 G) and an Oxford Instruments VSM (magnetisation *versus* field at 4 K).

Results and discussion

Since the 2 K NPD data allowed detailed investigation of both nuclear and magnetic structures, this paper focuses only on these data sets. However, the basic structural features were revealed by analysis of the ambient temperature data, and it is useful to summarise these prior to consideration of the detailed aspects of the low temperature data. Rietveld refinement of the ambient temperature NPD data confirmed that both Sr_2MnGaO_5 and Ca_2MnAlO_5 crystallise in the brownmillerite structure with alternate layers of MnO_6 octahedra and oxygen deficient layers of either GaO_4 or AlO_4 tetrahedra, respectively. The oxygen vacancies in these layers are ordered such that they result in the tetrahedra forming corner-linked chains running along the [001] direction. The arrangement of these chains within the brownmillerite structure corresponds to one of three possible space groups (*Icmm*, *Ibm*2 and *Pcmn*), which afford different displacements of the oxygen atoms within the layers of tetrahedral cations. In all symmetries, the chains of tetrahedra are fully ordered and directed along [001]. Although *Ibm*2 and *Pcmn* describe structures with similar cooperative rotations of the tetrahedra within a given layer (to achieve optimum metal–oxygen bond length criteria), adjacent tetrahedral layers have opposed oxygen displacements in *Pcmn*, which is centrosymmetric, but parallel displacements in the acentric *Ibm*2 space group. Since the separation between tetrahedral layers is around 8 Å, it is not surprising that long-range order between the layers may be absent, and the *Pcmn* and *Ibm*2 local order arrangements then transform to *Icmm*, for which split atom sites occur, corresponding to the two possible senses for cooperative displacements in a given layer (see Fig. 2; for more detail see Greaves *et al.*[6]).

Although the difference between the possible space groups is subtle, NPD data provided a clear differentiation. The results of the 300 K refinements for Sr_2MnGaO_5 confirmed that *Icmm* (R_{wp} = 2.23%, χ^2 = 3.30) was preferred in comparison to either *Ibm*2 (R_{wp} = 3.11%, χ^2 = 5.28) or *Pcmn* (R_{wp} = 3.56%, χ^2 = 8.560). Therefore, we can conclude that the GaO_4 chains, although always ordered along [001], are disordered with respect to the two possible chain orientations. This finding is in complete agreement with our previous observation for this phase, which was derived from the Rietveld analysis of X-ray powder diffraction data.[3] This NPD analysis also revealed a small degree of Mn–Ga mixing (~5%) and also provided a much lower thermal parameter for the tetrahedral cation site than was achieved in the fit to the X-ray diffraction data.

Our description of Sr_2MnGaO_5 based on *Icmm* symmetry disagrees with that of the X-ray powder diffraction study reported by Abakumov *et al.*,[9] where it is claimed that the structure is best represented by the space group *Ima*2 (or *Ibm*2), thus implying complete three-dimensional order in the arrangement of GaO_4 chains and incorporating identical chain displacements within a given GaO layer. Surprisingly, this appears to be inconsistent with the HREM study contained within the same report, where layers containing local areas of alternating GaO_4 chain orientations were suggested.[9] However, as acknowledged in the report by Abakumov *et al.*,[9] the space group assignment was a tentative one, based on the X-ray diffraction study alone and therefore we believe that our observation of bulk disorder in chain orientations, implied by space group *Icmm*, and now based on NPD, is a more reliable model and is also consistent with the aforementioned HREM study. Space group *Icmm* may also provide an improved description of the chain arrangement in Ca_2MnGaO_5 that Abakumov *et al.* have recently suggested is a mixture of phases of *Ibm*2 and *Pnma* symmetry.[10]

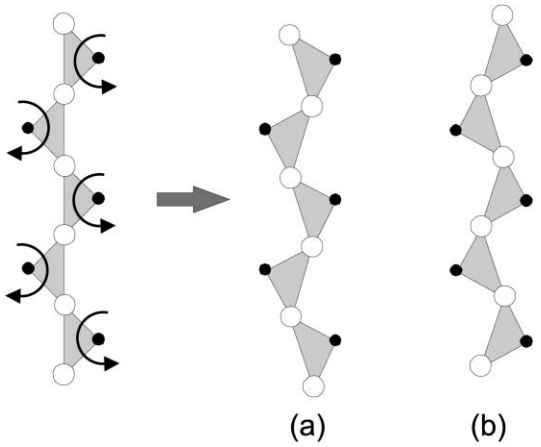

Fig. 2 Schematic of cooperative rotations of GaO_4 tetrahedra within a given layer to give the chain orientation (a). Reversed rotations would give the alternative orientation shown in (b).

In contrast to our studies on Sr_2MnGaO_5, the 300 K NPD data for Ca_2MnAlO_5 indicated the presence of fully ordered chains, with *Ibm*2 (R_{wp} = 2.14%, χ^2 = 2.99) clearly preferred to *Icmm* (R_{wp} = 6.90%, χ^2 = 27.5). The absence of any additional peaks consistent with primitive symmetry allowed *Pcmn* to be eliminated as a possible space group. In addition, no evidence supported Mn–Al mixing in Ca_2MnAlO_5.

Refinements for both phases indicated that the oxygen content was exactly 5.0 within one standard deviation, and the MnO_6 octahedra have elongation of the axial Mn–O bonds consistent with a Jahn–Teller distortion expected for Mn^{3+} cations.

Several factors may be involved in providing the higher degree of three-dimensional order observed in Ca_2MnAlO_5. Firstly, the presence of small amounts of Mn on the Ga sites in Sr_2MnGaO_5 is bound to disrupt the chain ordering; this effect is not observed in Ca_2MnAlO_5. It is also important to consider the smaller separation between the Al layers in Ca_2MnAlO_5 (7.5 Å) compared with the distance between Ga layers in Sr_2MnGaO_5 (8.1 Å), which will clearly influence interlayer chain order. We have also performed Madelung energy calculations,[14] as a guide to the lattice energies of the ordered chain orientation (*Ibm*2) and disordered chains (*Icmm*) for both Sr_2MnGaO_5 and Ca_2MnAlO_5. These calculations suggest that in pure enthalpy terms, the Sr_2MnGaO_5 ordered arrangement was 4574 kJ mol^{-1} more stable than the disordered one, whereas in Ca_2MnAlO_5 the difference was significantly greater with a value of 5900 kJ mol^{-1}. Although not conclusive, we can infer from these calculations that the ordered arrangement is more favoured on lattice enthalpy grounds in Ca_2MnAlO_5.

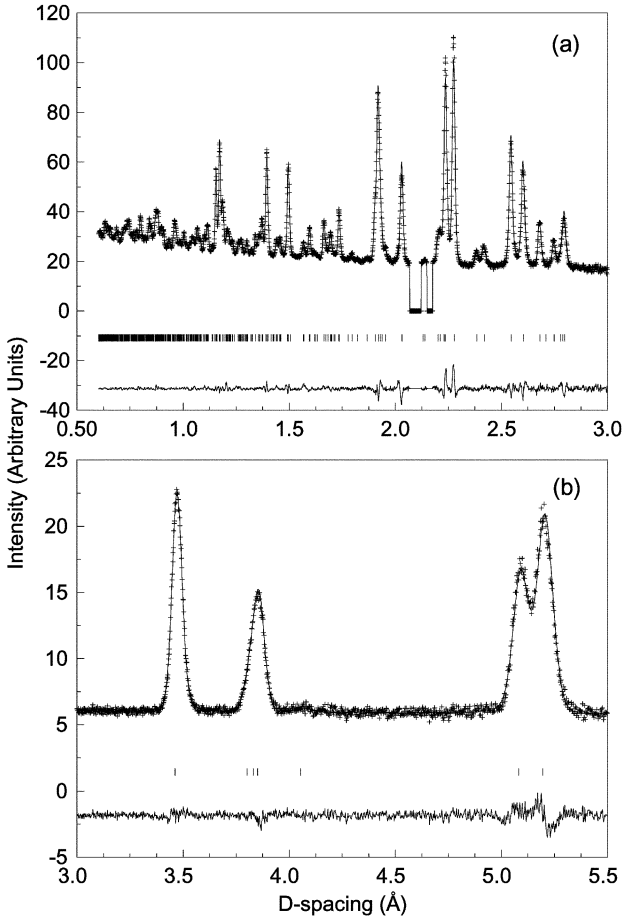

Fig. 3 Neutron powder diffraction profiles (continuous lines calculated and difference; crosses observed data) for Sr_2MnGaO_5 at 2 K. The tick marks indicate the reflection positions. The small additional peaks generated by the cryostat have been excluded. (a) Back scattering (C) bank data. (b) Low angle (A) bank data.

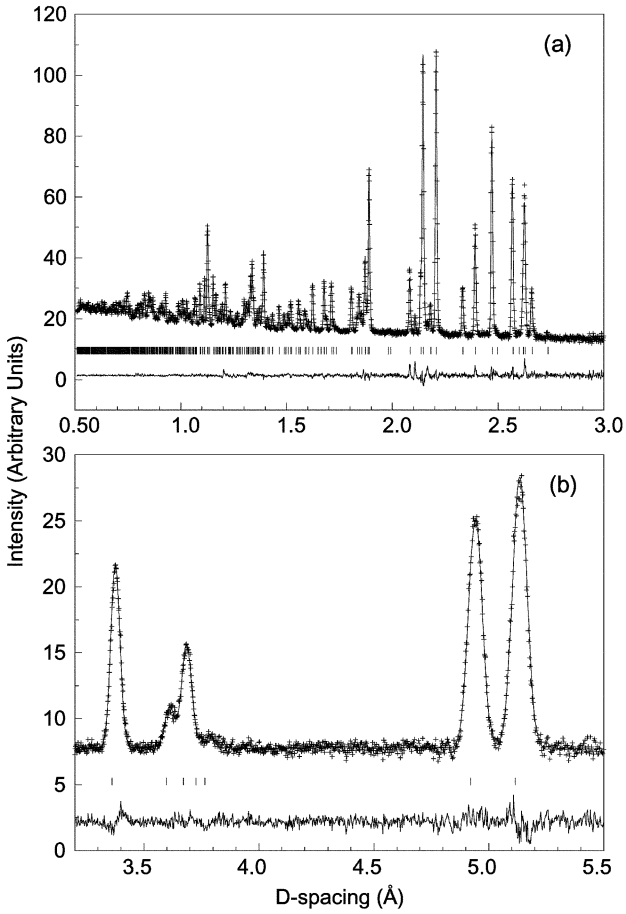

Fig. 4 Neutron powder diffraction profiles (continuous lines calculated and difference; crosses observed data) for Ca_2MnAlO_5 at 2 K. The tick marks indicate the reflection positions. (a) Back scattering (C) bank data. (b) Low angle (A) bank data.

The 2 K NPD data were analysed in order to investigate the ordering of the Mn^{3+} magnetic moments. The atomic positions, lattice parameters and space groups determined from the room temperature data were used as an initial model for these Rietveld refinements. The final refinement profiles for Sr_2MnGaO_5 and Ca_2MnAlO_5 are shown in Figs. 3 and 4, and the results of the refinements, together with selected bond distances and angles are shown in Tables 1–4. Weak peaks from the cryostat are responsible for the slightly poor fit in the vicinity of $d \approx 2.1$ Å for Ca_2MnAlO_5, Fig. 4. For Sr_2MnGaO_5, the peaks did not interfere with any structural peaks and were excluded from the refinement. The geometric arrangement of the MnO_6 octahedra and $Ga(Al)O_4$ tetrahedra are shown in Fig. 5. Table 1 shows that Sr_2MnGaO_5 has a small amount of mixing between the Mn and Ga cations ($\sim$5%); the thermal parameters and atomic coordinates for both cations on a given site were constrained to be equal. It was found that the Mn^{3+} ions order in an antiferromagnetic manner resulting in the magnetic space group *Icm′m′* for Sr_2MnGaO_5 and *Ibm′*2 for Ca_2MnAlO_5, as expected from simple superexchange coupling between Mn^{3+} ions. The moments are directed along [010] and [0–10] as shown in Fig. 6. The refined moments were 3.26(3) μ_B for Sr_2MnGaO_5 and 3.53(2) μ_B for Ca_2MnAlO_5 and are in good agreement with the expected moment for Mn^{3+} ions (free ion moment 4 μ_B).

Magnetic measurements were also carried out for these phases and were consistent with the findings from the Rietveld refinements. The magnetic behaviour of Sr_2MnGaO_5 has been previously reported;[3] although complex magnetic order was

Table 1 Refined structural parameters for Sr_2MnGaO_5 obtained from Rietveld analysis of neutron powder diffraction data (2 K)[a]

Atom	Site	Multiplicity	*x*	*y*	*z*	$U_{iso} \times 100/Å^2$	Occupancy
Sr	M(001)	8	0.5118(1)	0.11220(4)	0	0.30(2)	1
Mn1	2/M(001)	4	0	0	0	0.16(5)	0.953(3)
Ga1	2/M(001)	4	0	0	0	0.16(5)	0.047(3)
Mn2	M(100)	8	0.0704(2)	0.25	−0.0433(3)	0.85(5)	0.023(2)
Ga2	M(100)	8	0.0704(2)	0.25	−0.0433(3)	0.85(5)	0.477(2)
O1	2(100)	8	0.25	0.00490(8)	0.25	0.60(2)	1
O2	1	16	−0.0410(2)	0.14567(6)	0.0123(8)	0.65(4)	0.5
O3	M(100)	8	0.3751(4)	0.25	0.8897(4)	0.77(5)	0.5

[a] $R_{wp} = 1.37\%$, $R_p = 2.25\%$, $R_F^2 = 2.05\%$, $R_{mag} = 1.17\%$, $\chi^2 = 2.895$. *Icmm*: $a = 5.4888(2)$ Å, $b = 16.2256(6)$ Å, $c = 5.35450(2)$ Å. *Icm′m′*: Mn |Moment| = 3.26(3) μ_B.

Table 2 Selected bond lengths (Å) and bond angles (°) for Sr_2MnGaO_5

Mn1/Ga1–O1	1.91872(7)[×4]	Sr–O1	2.625(1) [×2], 2.667(1) [×2]
Mn1/Ga1–O2	2.375(1) [×4]	Sr–O2	2.515(1), 2.672(4), 2.801(4), 3.083(1)
Ga2/Mn2–O2	1.824(1) [×2]	Sr–O3	2.431(1), 3.723(2)
Ga2/Mn2–O2	1.808(1) [×2]		
Ga2/Mn2–O3	1.710(2), 1.863(2), 1.879(3), 2.338(3)		
O1–Mn1/Ga1–O1	88.490(4)		
O1–Mn1/Ga1–O1	180.0		
O1–Mn1/Ga1–O1	91.510(4)		
O1–Mn1/Ga1–O2	91.51(5)		
O1–Mn1/Ga1–O2	180.0(2)		
O1–Mn1/Ga1–O2	88.5(2)		
O2–Ga2/Mn2–O2	136.2(2), 137.77(9)		
O2–Ga2/Mn2–O3	98.3(2), 102.4(1), 103.23(8), 105.24(9), 110.5(2), 111.2(2)		
O3–Ga2/Mn2–O3	107.03(9), 68.72(3)		

Table 4 Selected bond lengths (Å) and bond angles (°) for Ca_2MnAlO_5

Mn–O1	1.888(2) [×2]	Ca–O1	2.486(1), 2.555(1), 2.583(1), 2.512(1)
Mn–O1	1.909(2) [×2]	Ca–O2	2.296(1), 2.498(1), 2.863(1), 3.290(1)
Mn–O2	2.249(1) [×2]	Ca–O3	2.352(1), 3.544(1)
Al–O2	1.744(1) [×2]		
Al–O3	1.793(2)		
Al–O3	1.799(2)		
O1–Mn–O1	92.6(1)	O2–Al–O2	121.9(1)
O1–Mn–O1	179.66(1)	O2–Al–O3	106.5(1)
O1–Mn–O1	87.07(1)	O2–Al–O3	107.0(1)
O1–Mn–O1	93.3(1)	O2–Al–O3	106.5(1)
O1–Mn–O2	85.8(6)	O2–Al–O3	107.0(1)
O1–Mn–O2	88.91(6)	O3–Al–O3	107.0(1)
O1–Mn–O2	91.20(1)		
O1–Mn–O2	94.17(1)		
O2–Mn–O2	172.22(6)		

implied, it is based on the antiferromagnetic order shown in Fig. 6. It was thought that the anomaly in the behaviour of this material was due to small ferromagnetic regions, and was tentatively attributed to domains with *Ibm*2 order, for which a small canting of the Mn moments is possible. Mass susceptibility data were collected for Ca_2MnAlO_5 (Fig. 7) and show a divergence in the zero field and field cooled data. This suggests both antiferromagnetic and ferromagnetic components of magnetic order below a critical temperature $T_N = 152$ K, as is often observed in materials with a canted antiferromagnetic arrangement of magnetic spins. This is consistent with the powder neutron data since small angles of canting would not be apparent from powder data and only the predominant antiferromagnetic order would be revealed. This is also true for Sr_2MnGaO_5. It is also of interest to note that for the fully ordered (*Ibm*2) Ca_2MnAlO_5, the canting of spins is readily apparent in the magnetic susceptibility data. This lends more weight to the argument that the anomaly in the data for Sr_2MnGaO_5 is indeed due to localised regions of *Ibm*2 order with canted moments. Magnetisation data as a function of field at 4.2 K were also collected for Ca_2MnAlO_5 (Fig. 8). These data show that the magnetic moment for this material does not saturate even at 10 T. This is again consistent with the canting of the magnetic moments.

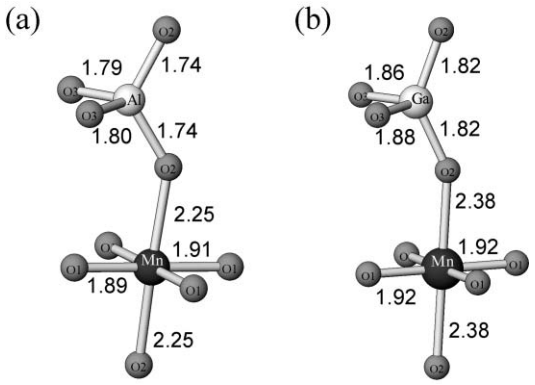

Fig. 5 Localised coordination environments, including bond lengths, of (a) Al and Mn in Ca_2MnAlO_5 and (b) Ga and Mn in Sr_2MnGaO_5 (this representation is based on the fully ordered *Ibm*2 structure to aid clarity). More accurate bond distances are in Tables 2 and 4.

Conclusions

The brownmillerite phases, Sr_2MnGaO_5 and Ca_2MnAlO_5 have been successfully synthesised and full structural characterisation achieved using neutron powder diffraction data. Whereas Sr_2MnGaO_5 crystallises in space group *Icmm* and does not show completely ordered displacements within the chains of tetrahedra, Ca_2MnAlO_5 crystallises in the fully ordered space group *Ibm*2. A slightly improved fit to the data for Sr_2MnGaO_5 was found to be achieved by allowing a small amount of Mn–Ga mixing ($\sim$5%). Rietveld refinement of low temperature powder neutron diffraction data revealed that both phases showed antiferromagnetically ordered Mn^{3+} moments. Magnetic measurements were consistent with the neutron data, but in addition showed both phases to have more complex order due to canting of the magnetic moments.

The brownmillerite structure has potential for providing a new family of CMR materials, and the materials described here are of considerable interest. In this respect, it is relevant to note that it is also possible to control the oxygen non-stoichiometry in both the phases discussed here. This allows chemical control of the Mn oxidation state and hence the magnetic and electronic properties of the materials. A full report of the phases with higher oxygen contents will follow. If this control of the Mn oxidation state was combined with the synthesis of the higher members of this family of materials ($A_{n+1}Mn_n(Ga/Al)O_{3n+2}$) the phases produced should have great potential as low field CMR materials.

Table 3 Refined structural parameters for Ca_2MnAlO_5 obtained from Rietveld analysis of neutron powder diffraction data (2 K)[a]

Atom	Site	Multiplicity	x	y	z	$U_{iso} \times 100/Å^2$	Occupancy
Ca	1	8	0.5266(2)	0.11181(6)	0.0069(2)	0.51(2)	1
Mn	2(001)	4	0	0	0	0.63(3)	1
Al	M(100)	4	0.0732(3)	0.25	0.0415(3)	0.24(3)	1
O1	1	8	0.2479(2)	0.01151(5)	0.2496(2)	0.38(1)	1
O2	1	8	−0.0664(1)	0.14807(5)	−0.0290(2)	0.62(2)	1
O3	M(100)	4	0.3620(2)	0.25	0.8785(2)	0.47(2)	1

[a] $R_{wp} = 1.05\%$, $R_p = 1.82\%$, $R_F^2 = 2.38\%$, $R_{mag} = 2.40\%$, $\chi^2 = 1.88$. *Ibm*2: $a = 5.46258(9)$ Å, $b = 14.9533(3)$ Å, $c = 5.23135(8)$ Å. *Ibm*′2: Mn |Moment| = 3.53(2) μ_B.

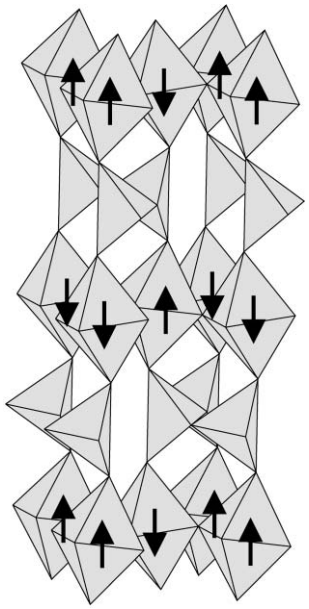

Fig. 6 Antiferromagnetic structure of Sr_2MnGaO_5 and Ca_2MnAlO_5.

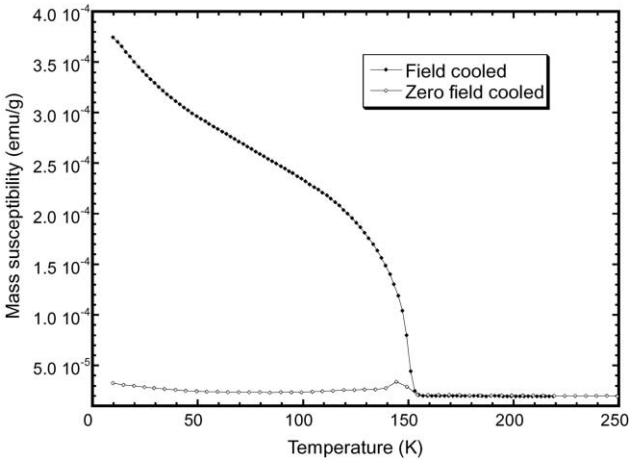

Fig. 7 Mass susceptibility against temperature data for Ca_2MnAlO_5 (magnetic field 500 G).

Acknowledgement

We thank EPSRC for financial support and the provision of neutron diffraction facilities. We are grateful to Dr Ron Smith for his assistance in the collection of neutron diffraction data.

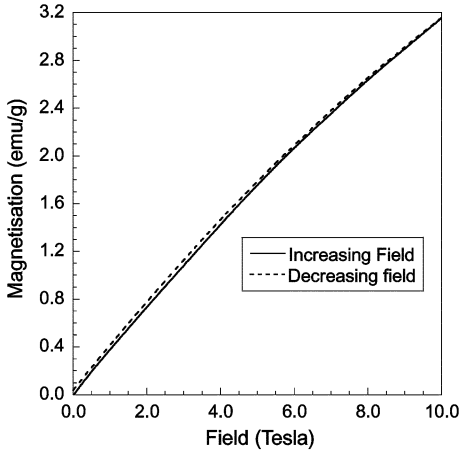

Fig. 8 Magnetisation against field data for Ca_2MnAlO_5 (4.2 K).

References

1 Y. Moritomo, A. Asamitsu, H. Kuwahar and Y. Tokura, *Nature*, 1996, **380**, 141.
2 P. D. Battle and M. J. Rosseinsky, *Curr. Opin. Solid State Mater. Sci.*, 1999, **4**, 163.
3 A. J. Wright, H. M. Palmer, P. A. Anderson and C. Greaves, *J. Mater. Chem.*, 2001, **11**, 1324.
4 E. F. Bertaut, P. Blum and A. Sagnieresn, *Acta Crystallogr.*, 1959, **12**, 149.
5 P. Berastegui, S.-G. Eriksson and S. Hull, *Mater. Res. Bull.*, 1999, **34**, 303.
6 C. Greaves, A. J. Jacobson, B. C. Tofield and B. E. F. Fender, *Acta Crystallogr., Sect. B*, 1975, **31**, 641.
7 V. M. Harder and Hk. Muller-Buschbaum, *Z. Anorg. Allg. Chem.*, 1980, **464**, 169.
8 S. Geller, R. W. Grant and L. D. Fuller, *J. Phys. Chem. Solids*, 1970, **31**, 793.
9 A. M. Abakumov, M. G. Rozova, B. Ph. Pavlyuk, M. V. Lobanov, E. V. Antipov, O. I. Lebedev, G. Van Tendeloo, O. L. Ignatchik, E. A. Ovtchenkov, Yu. A. Koksharov and A. N. Vasil'ev, *J. Solid State Chem.*, 2001, **160**, 353.
10 A. M. Abakumov, M. G. Rozova, B. Ph. Pavlyuk, M. V. Lobanov, E. V. Antipov, O. I. Lebedev, G. Van Tendeloo, D. V. Sheptyakov, A. M. Balagurov and F. Bourée, *J. Solid State Chem.*, 2001, **158**, 100.
11 F. Puertas, M. T. Blanco Varela and R. Dominguez, *Cem. Concr. Res.*, 1990, **20**, 429.
12 A. C. Larson and R. B. Von Dreele, General Structure Analysis System, Los Alamos National Laboratory, 1994.
13 R. E. Watson and A. T. Freeman, *Acta Crystallogr.*, 1961, **14**, 27.
14 J. W. Weenk and H. A. Harwig, *J. Phys. Chem. Solids*, 1977, **38**, 1047.